1521-009X/50/9/1182–1189$35.00
DRUG METABOLISM AND DISPOSITION
dx.doi.org/10.1124/dmd.122.000900
Drug Metab Dispos 50:1182–1189, September 2022

High-Throughput Production of Diverse Xenobiotic Metabolites with Cytochrome P450–Transduced Huh7 Hepatoma Cell Lines[S]

Choon-myung Lee, Ken H. Liu, Grant Singer, Gary W. Miller, Shuzhao Li, Dean P. Jones, and Edward T. Morgan

Department of Pharmacology and Chemical Biology, Emory University School of Medicine, Atlanta, Georgia (C.-m.L., G.S., E.T.M.); Clinical Biomarkers Laboratory, Department of Medicine, Emory University, Atlanta, Georgia (K.H.L., D.P.J.); Department of Environmental Health Sciences, Columbia University Mailman School of Public Health, New York, New York (G.W.M.); and The Jackson Laboratory for Genomic Medicine, Farmington, Connecticut (S.L.)

Received March 15, 2022; accepted June 1, 2022

ABSTRACT

Precision medicine and exposomics require methods to assess xenobiotic metabolism in human metabolomic analyses, including the identification of known and undocumented drug and chemical exposures as well as their metabolites. Recent work demonstrated the use of high-throughput generation of xenobiotic metabolites with human liver S-9 fractions for their detection in human plasma and urine. Here, we tested whether a panel of lentivirally transduced human hepatoma cell lines (Huh7) that express individual cytochrome P450 (P450) enzymes could be used to generate P450-specific metabolites in a high-throughput manner, while simultaneously identifying the enzymes responsible. Cell-line activities were verified using P450-specific probe substrates. To increase analytical throughput, we used a pooling strategy where 36 chemicals were grouped into 12 unique mixtures, each mixture containing 6 randomly selected compounds, and each compound being present in two separate mixtures. Each mixture was incubated with 8 different P450 cell lines for 0 and 2 hours and extracts were analyzed using liquid chromatography–high-resolution mass spectrometry. Cell lines selectively metabolized test substrates, e.g., pazopanib, bupropion, and β-naphthoflavone with expected substrate-enzyme specificities. Predicted metabolites from the remaining 33 compounds as well as many unidentified *m/z* features were detected. We also showed that a specific bupropion metabolite generated by CYP2B6 cells, but not detected in the S9 system, was identified in human samples. Our data show that the chemical mixtures approach accelerated characterization of xenobiotic chemical space, while simultaneously identifying enzyme sources that can be used for scalable generation of metabolites for their identification in human metabolomic analyses.

SIGNIFICANCE STATEMENT

High-resolution mass spectrometry (HRMS) enables the detection of exposures to drugs and other xenobiotics in human samples, but chemical identification can be difficult for several reasons. This paper demonstrates the utility of a panel of engineered cytochrome P450–expressing hepatoma cells in a scalable workflow for production of xenobiotic metabolites, which will facilitate their use as surrogate standards to validate xenobiotic detection by HRMS in human metabolomic studies.

Introduction

Widespread use of high resolution mass spectrometry (HRMS)-based metabolomics methods shows that many unidentified mass spectral features are significantly associated with human diseases, with many features likely arising from undocumented drug, dietary supplement and environmental chemical exposures (Jones, 2016; Uppal et al., 2016). Despite advancements in instrumentation and bioinformatic tools for chemical annotation (Uppal et al., 2017; Blaženović et al., 2019) and prediction of biotransformation (Djoumbou-Feunang et al., 2019), the lack of authentic standards for xenobiotic metabolites is an obstacle for identification of xenobiotic exposures. Developing a high-throughput platform for generation of biotransformation products for thousands of xenobiotic chemicals would establish experimentally validated sets of xenobiotic metabolites that could be used for identification of undocumented exposures in people.

We recently used human liver S9 fractions to develop an in vitro high-throughput biotransformation platform coupled with HRMS, showing that generated xenobiotic metabolites can be used as reference mixtures to identify xenobiotic exposures in human blood and urine (Liu et al., 2021). However, one disadvantage of using S9 fractions for biotransformation is that not all xenobiotic metabolizing enzymes are equally expressed. As a result, the metabolic contributions of enzymes that are less highly expressed or that have lower specific activity may be missed. In the present study, we used lentiviral transduction to develop a panel of cytochrome P450 (P450)–expressing Huh7 hepatoma cell lines, each expressing a specific P450. P450s are a gene superfamily of monooxygenases that are universal in all living systems.

This work was supported by the National Institutes of Health of Environmental Health Science [Grant U2C-ES030163] (to G.W.M., S.L., D.P.J., E.T.M.) and [Grant 1P30-ES019776] (D.P.J., E.T.M).

No author has an actual or perceived conflict of interest with the contents of this article.

A preprint of this article was deposited in bioRxiv [https://doi.org/10.1101/2022.03.12.484071].

dx.doi.org/10.1124/dmd.122.000900.

[S] This article has supplemental material available at dmd.aspetjournals.org.

ABBREVIATIONS: ACN, acetonitrile; C18, reverse phase chromatography; CLZ, chlorzoxazone; DMEM, Dulbecco's modified Eagle medium; ESI, electrospray ionization; HILIC, hydrophilic interaction liquid chromatography; HRMS, high-resolution mass spectrometry; LC, liquid chromatography; β-NF, β-naphthoflavone; P450, cytochrome P450; PS, penicillin/streptomycin; RT, retention time.

Mammalian P450s are involved in oxidation of many substrates including fatty acids, steroids, and xenobiotics. Although there are 18 families with 57 P450 genes in humans, P450 families 1 through 3 are mainly involved in xenobiotic metabolism such as drugs, food nutrients, environmental chemicals, etc. (Nebert et al., 2013). Moreover CYP1, 2, 3 families are involved in metabolism of more than half of clinically available drugs (Cerny, 2016). We used these cell lines as a complement to the generalized S9 system to allow for simultaneous production of xenobiotic metabolites and identification of specific enzyme(s) that are capable of producing them. The identification of substrate-enzyme pairs would allow specific P450 metabolites of interest to be scaled-up for additional characterization and facilitate the identification of xenobiotic exposures in human samples.

In validation and testing, we recognized liquid chromatography (LC)-HRMS throughput as a bottleneck to large-scale characterization of xenobiotic metabolites, and so we tested a mixture's metabolism workflow with these P450 cell lines to address this limitation. Thirty-six chemicals were grouped into 12 mixtures of 6 randomly selected compounds, with each compound present in two separate mixtures. These 12 individual mixtures were incubated with 8 different cytochrome P450-expressing Huh7 cell lines, with cell extracts collected and analyzed using LC-HRMS. Our data show that adoption of this workflow increased analytic throughput by a factor of six, and also demonstrate the formation of unexpected metabolites in a cell-line–specific manner. In doing so, we establish that this cell-line–based platform provides a scalable approach for generating and identifying xenobiotic metabolites that is complementary to the previously described S9 platform (Liu et al., 2021), expanding the coverage of chemical space for identification of xenobiotic exposures in human exposomics.

Materials and Methods

Materials. Acenaphthene, acetaminophen, auranofin, β-naphthoflavone (β-NF), benzo[a]pyrene, bupropion, caffeine, chlorzoxazone (CLZ), nicotine, tolbutamide, trifluralin, naphthalene, coumarin, fluoranthene, 1,2-diphenylhydrazine, ethylbenzene, 2,4,6-trichlorophenol, estrone, 1,1,2,2-tetrachloroethane, N-nitrosodipropylamine, 2-methylnaphthalene, endrin aldehyde, azinphos-methyl, dexamethasone, Geneticin (G418), pazopanib, S,S,S tributyl-phosphorotrithioate, bromodichloromethane, ethion, benzo[b]fluoranthene, bis(2-ethylhexyl)phthalate, crizotinib, 1,2-dichlorobenzene, o,p'- dichlorodiphenyldichloroethane (DDD), omeprazole, pazopanib, polybrene, warfarin, and HPLC grade acetonitrile were purchased from Sigma-Aldrich (St. Louis, MO). S,S-hydroxy and R,R-hydroxy bupropion were purchased from Cayman Chemical, Ann Arbor, MI) and vandetanib was from AstaTech (Bristol, PA). Blasticidin was obtained from InvivoGen (San Diego, CA). Rabbit anti-V5 (V8137), mouse anti-glyceraldehyde 6-phosphate dehydrogenase (MAB374), and mouse anti-actin (A2228) antibodies were purchased from Sigma.

Generation of P450 Expressing Cell Lines and Immunoblotting. Human hepatoma Huh7 cell lines individually expressing CYP1A2, 2A6, 2B6, 2C8, 2C19, 2D6, 2E1, or 3A4 with a C-terminal V5 tag were generated as described in previous studies (Park et al., 2017; Cerrone et al., 2020; Lee et al., 2020). The lentiviral vector pLX304-2D6 (cat# EX-A3525-LX304) was purchased from GeneCopoeia (Rockville, MD). The other lentiviral vectors (pLX304-CYP) were obtained from the DNASU plasmid repository center. pLX304 plasmids with cloned V5-tagged P450s were transfected together with a second-generation lentiviral packaging system consisting of pMD2.G and psPAX2 plasmids into HEK293T cells to generate virus particles. Forty-eight and 72 hours after transfection, media containing virus particles were collected and filtered through a 0.45 μm filter, and stored at −80°C. Huh7 cells were infected with viral media containing 10% fetal bovine serum (FBS)/1% penicillin/streptomycin (PS)/Dulbecco's modified Eagle medium (DMEM) and polybrene (8 μg/ml) to enhance transduction. Cells were selected with 10 μg/ml blasticidin beginning at 24 hours after infection.

To confirm the expression of the individual P450s, the cells were grown to 95–100% confluence and the proteins were extracted with cell lysis buffer. The total cell lysates were collected and centrifuged at 12,000 × g for 5 minutes and then the supernatant was collected and prepared for SDS-PAGE. Immunoblotting was carried out using anti-V5 antibodies (1:5000; Sigma) as described previously (Cerrone et al., 2020).

P450 Activity Time Course Assays. The eight P450 cell lines were plated on 96-well plates in 10% FBS/1% PS/10 μg/mL blasticidin/DMEM media until they reached 100% confluency. After media were removed, 50 μL of media containing a mixture of seven P450 substrates (20 μM each of 7-ethoxyresorufin (CYP1A2), coumarin (CYP2A6), bupropion (CYP2B6), amodiaquine (CYP2C8), omeprazole (CYP2C19 and 3A4), dextromethorphan (CYP2D6), and chlorzoxazone (CYP2E1) were added to the wells and incubated for the indicated time. The incubations were stopped by addition of 150 μL of acetonitrile, mixed by repetitive pipetting, and centrifuged at 3000 × g for 5 minutes. The supernatants were transferred into 96-well liquid chromatography (LC)-ready plates for LC-HRMS analysis.

Pooling Strategy to Improve Throughput for Xenobiotic Metabolite Generation. Thirty-six chemicals were grouped into 12 separate mixtures at a final concentration of 20 μM in 1% dimethylsulfoxide. Each pool contained 6 randomly assigned compounds (so that each chemical would be present in 2 distinct mixtures) in P450 assay buffer (1 mM Na_2HPO_4, 137 mM NaCl, 5 mM KCl, 0.5 mM $MgCl_2$, 2 mM $CaCl_2$, 10 mM glucose, and 10 mM Hepes, pH 7.4 (Donato et al., 2004). The eight cell lines expressing individual P450 enzymes were cultured in 10% FBS/1% PS/10/10 μg/mL blasticidin/DMEM media until they reached 100% confluency on 96-well plates. After removing media, each cell line was incubated with 50 μL of each of the 12 substrate pools in P450 assay buffer in two 96-well plates for 0 and 2 hours resulting in 192 samples for analysis. Reactions were terminated by addition of 150 μL of acetonitrile and processed as described above for LC-HRMS. In designing this pooling strategy, our criteria of having each compound in two different pools and that each compound would be the only one shared compound between its two pools was most easily achievable by using a number of substrates (n) equal to a perfect square, where the number of pools = $\sqrt{}$n*2 and the number of compounds in each pool = $\sqrt{}$n. In a 96 well (12x8) plate format 12 pools of 6 was a facile and consistent approach.

LC-HRMS. 10 μL aliquots of sample extracts were analyzed using liquid chromatography coupled to Orbitrap-based MS analysis (Dionex Ultimate 3000, Thermo Scientific Fusion or Thermo Scientific High-Field Q-Exactive). The chromatography system was operated in a dual pump configuration which allows sample analysis on one column with a second column undergoing flushing and reequilibration in parallel. Sample extracts were injected and analyzed using hydrophilic interaction liquid chromatography (HILIC) with electrospray ionization (ESI) operated in positive mode and reverse phase (C18) chromatography with ESI operated in negative mode. Analyte separation for HILIC was accomplished using a Waters XBridge BEH Amide XP HILIC column (2.1 mm × 50 mm, 2.5 μM particle size) and eluent gradient (A = water, B = acetonitrile, C = 2% formic acid) consisting of an initial 1.5-minute period of 22.5% A, 75% B, 2.5% C, followed by a linear increase to 75% A, 22.5% B, 2.5% C at 4 minutes and a final hold of 1 minute. C18 chromatography was performed using an endcapped C18 column (Higgins Targa C18 2.1 mm × 50 mm, 3 μM particle size) and gradient (A = water, B = acetonitrile, C = 10 mM ammonium acetate) consisting of an initial 1-minute period of 60% A, 35% B, 5% C, followed by a linear increase to 0% A, 95% B, 5% C at 3 minutes and held for the remaining 2 minutes. For both methods, mobile phase flow rate was held at 0.35 mL/min for the first 1 minute, increased to 0.4 mL/min for the final 4 minutes. Mass spectrometers were operated at 120,000 resolution and data were collected from 85-1,275 *m/z* for MS1 analysis with data-dependent MS/MS analyses performed at 60,000 resolution for MS1 and 30,000 resolution for MS2 using an inclusion list for predicted xenobiotic metabolites.

Identification of m/z Features. Raw data were processed in mzMine2 (Pluskal et al., 2010). Extracted data were organized into a feature table data file where each ion feature is represented by its characteristic *m/z*, retention time (RT), and associated peak intensity. Lists of accurate mass *m/z* ions for expected metabolites (M+H for HILIC+ and M-H for C18-) were generated in three complementary ways: from the literature, using Biotransformer (Djoumbou-Feunang et al., 2019) and by subtracting the exact mass of the parent compound from observed masses that increased with time and looking for discrete masses that corresponded to known biotransformations (demethylation, hydroxylation, etc.). These target lists were used to search the feature table for biotransformation

products for each precursor compound and metabolite peak intensities increased at 2 hours relative to 0-hour time points.

Results

Expression of Active, Tagged P450s and Characterization of Their Substrate Specificities

After selecting lentivirus transformed cells with blasticidin, we carried out immunoblotting with an anti-V5 antibody to confirm the expression of P450 proteins (Fig. 1). All P450 cell lines expressed the corresponding proteins with the C-terminal V5 tag. To examine the functionality and substrate specificity of the expressed enzymes, all cell lines were incubated for 0, 2, 4 and 6 hours with a mixture of 7 enzyme-selective substrates, and contents (cells and media) of each well were extracted and analyzed on the high-resolution mass spectrometer (Fig. 2). Huh7 cell lines, each labeled according to the specific P450 used for transfection (1A2, 2A6, 2B6, 2C8, 2C19, 2D6, 3A4), demonstrated robust substrate-selective activities (Fig. 2). The well-documented CYP1A substrate 7-ethoxyresorufin (Ghosal et al., 2003) was O-deethylated by the Huh7-CYP1A2 cell line to form resorufin (Fig. 2A) and the CYP2A6-specific substrate coumarin (Pelkonen et al., 2000) was oxidized only by the Huh7-CYP2A6 cell line to form 7-hydroxycoumarin (Fig. 2B). Huh7-CYP2B6 cells oxidized the CYP2B6-specific substrate bupropion (Hsyu et al., 1997) to hydroxybupropion (Fig. 2C). Additionally, we estimated the concentration of generated hydroxybupropion with the R,R-hydroxy bupropion standard (Fig. 3). Hydroxybupropion was generated rapidly within 4 hours and continued to be produced until 24 hours (Fig. 3B). At 24 hours, half of the added 10 mM buproprion had been converted to hydroxybupropion (Fig. 3B), showing the utility of this cell line to generate xenobiotic metabolites in large quantities. The CYP2B6 cell line also produced dihydroxybupropion from bupropion, although it was observed at 10-fold lower relative abundance compared with hydroxybupropion (Fig. 3C). Dihydroxybupropion was previously detected in human urine, but its metabolic source was unknown (Petsalo et al., 2007). Furthermore, we observed dihydroxybupropion in mice following oral gavage of bupropion (Fig. 4A), and in a plasma sample from a patient with documented bupropion use in which we had previously identified hydroxybupropion and hydrobupropion (Liu et al., 2021). The retention times and ion fragmentation spectra for dihydroxybupropion detected in the patient matched that of the CYP2B6 generated dihydroxybupropion (Fig. 4B).

A well-established CYP2C8 substrate amodiaquine (Li et al., 2002) was N-deethylated by the CYP2C8 cell line producing two forms of desethylamodiaquine (RT, 0.501 and 0.856 minute) in a time-dependent manner (Fig. 2D). Omeprazole was oxidized by two cell lines, CYP2C19 and CYP3A4 as expected (Yamazaki et al., 1997; Li et al., 2005) (Fig. 2E). However, CYP3A4 cells were 4.5-fold more active than CYP2C19 cells. Dextromethorphan is well a known probe drug for human CYP2D6 activity (Yu and Haining, 2001), and the CYP2D6 cell lines actively metabolized dextromethorphan to desmethyldextromethorphan (probably O-demethylation to dextrorphan) at 4 and 6 hours, while no product was detected at 2 hours (Fig. 2F). An additional experiment showed that the CYP2D6 cell line actively demethylated dextromethorphan within 2h (Supplemental Fig. 1A), as well as generating hydroxydesmethyldextrorphan (Supplemental Fig. 1B). Our data suggest that the CYP2D6 cell line is more active in hydroxylation of desmethyl dextromethorphan than dextromethorphan because we did not detect the hydroxydextromethorphan. Our initial experiment did not detect the CYP2E1 probe drug chlorzoxazone (CLZ) parent compound or hydroxychlorzoxazone formation by CYP2E1 cell lines when using the substrate mixture. However, a second experiment using CLZ as the lone substrate showed the time-dependent generation of OH-CLZ by CYP2E1 cells detected in C18 negative mode (Fig. 2G), suggesting inhibition of activity by other drugs or drug metabolites in the mixture. The data show that these P450-expressing cell lines have robust cell-line–specific (P450 specific) reactions and can be used for drug metabolism studies with some potential for interference when assayed as mixtures.

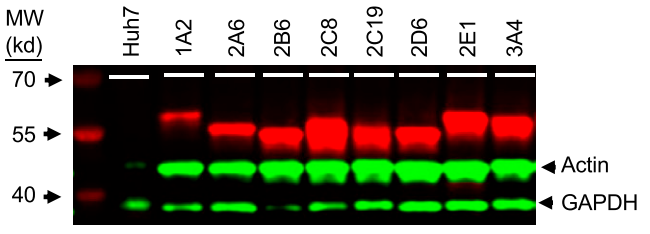

Fig. 1. Immunoblotting of P450 expressing cell lines. Equal volumes of total cell extracts from the indicated cell lines were separated on SDS-PAGE and blotted with anti-V5, anti-actin, and anti-GAPDH primary antibodies.

Cell-Line–Specific Metabolite Production From Pooled Mixtures

The above experiments using pooled probe substrates suggest that a substrate pooling strategy may facilitate efficient screening of large numbers of chemicals for metabolite production. We chose 36 compounds (Supplemental Table 1) to test this hypothesis, which included several chemicals with relatively well-characterized metabolites for validation and a range of xenobiotics selected from the ATSDR substance priority list. The 36 chemicals were pooled randomly into 12 pools with 6 individual compounds in a pool (Fig. 5; details provided in Supplemental Fig. 2) and each pool was incubated separately with each of the 8 P450-expressing cell lines for 0 and 2 hours prior to analysis by LC-HRMS. The resulting complex data (Fig. 6; Table 1) were simplified by targeted searching for predicted metabolites as well as application of data tools to search for other nonpredicted products; selected examples are provided to illustrate the utility of the cell lines for generation of products to aid in metabolite identification in human metabolomics studies and also to discover an uncharacterized metabolite.

Examples of Specific Xenobiotics. Results for two well-studied drugs, tolbutamide and pazopanib, are shown in Fig. 6. Hydroxytolbutamide (Wester et al., 2000) was generated only by the CYP2C19 cell line in pools containing tolbutamide. Pazopanib is mainly metabolized by CYP3A4 and to a minor degree by CYP1A2 and 2C8 based on a previous *in vitro* study (Keisner and Shah, 2011). We detected hydroxypazopanib following incubations with CYP3A4 and CYP2C8 cells (and at significantly lower levels in one of the two CYP1A2 cell line incubations). Desmethyl pazopanib was generated only from CYP3A4 and CYP2C8 cell lines (Fig. 6). Similarly, hydroxy β-NF was detected only in incubations of the CYP1A2 cell line with pools containing β-NF (Pool 1 and Pool 12) shown here using C18 LC and negative ionization mode (Fig. 6). These data show that predicted metabolites were generated in a cell line specific manner from pooled mixtures, which verifies that a mixtures approach can be used with these cell lines to generate and detect xenobiotic metabolites.

Evidence for unidentified metabolites. Trifluralin is one of most widely used herbicides in the environment, whose health hazards are not known (https://www.epa.gov/sites/production/files/2016-09/documents/trifluralin.pdf). Identifying potential health risks associated with trifluralin exposure requires confident detection in human exposome studies. However, to the best of our knowledge, human P450 trifluralin metabolism is not characterized, which limits our ability to identify these exposures in human samples. Our experiments with trifluralin showed the generation of three features with m/z 260.0640, 290.0744, and 368.1059 by CYP2B6 and CYP2E1 cell lines (Fig. 6).

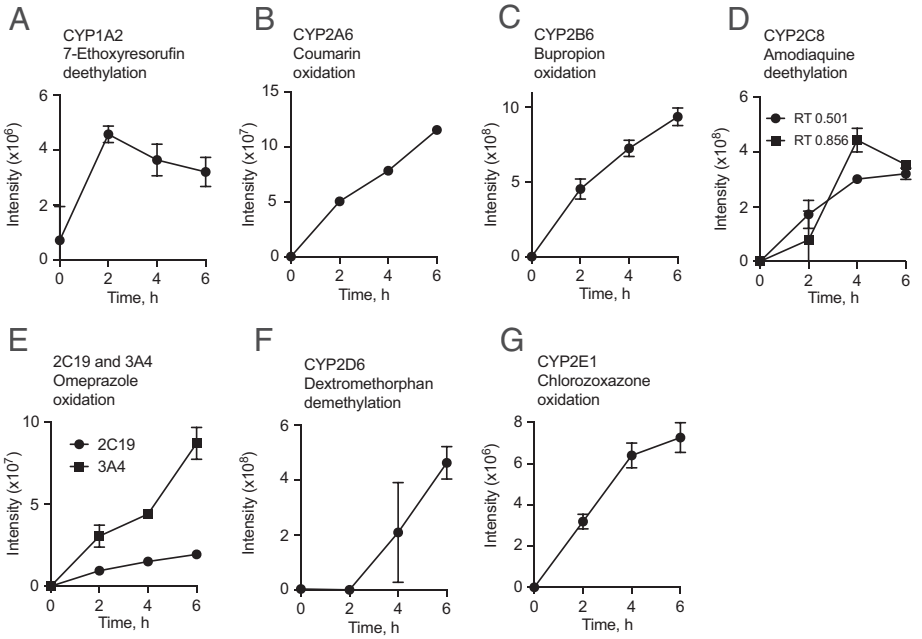

Fig. 2. Cell line and substrate specificity. A mixture of 7 substrates at 20 μM final concentration were incubated with each P450-expressing cell line for the indicated times, quenched with 3 volumes of acetonitrile (ACN), and then analyzed by LC-HRMS (Q Exactive HF mass spectrometer). Only detected signals were plotted. The predicted product masses were selected by 3 criteria: 1) mass (*m/z*) tolerance should be within 0.0005, 2) masses should have the same retention time, and 3) the signal should increase over time. All signals were detected in HILIC positive mode except chlorzoxazone in *panel G* where the signal was detected in C18 negative mode. (A) Ethoxyresorufin deethylation (BROD) by CYP1A2 cell line; (B) coumarin hydroxylation by CYP2A6 cell line; (C) bupropion hydroxylation by CYP2B6 cell line; (D) amodiaquine deethylation by CYP2C8; (E) omeprazole hydroxylation by CYP2C19 and 3A4 cell lines; (F) dextromethorphan demethylation by CYP2D6; (G) chlorzoxazone (CLZ) hydroxylation by CYP2E1 (C18). CYP2E1 cell lines were incubated with only chlorzoxazone for the indicated time and analyzed on the same LC-HRMS since we were not able to detect the OH-CLZ from the mixed substrate samples. Values are means ± S.D. of three individual wells from the same cell preparation.

The intensities at 290.0744, and 368.1059 were relatively high, while the *m/z* 260.0640 metabolite was generated from both cell lines at significantly lower levels. 368.1059 *m/z* is consistent with dihydroxytrifluralin, and MS/MS spectra are also consistent with this annotation (data not shown). However, the chemicals associated with 290.0744 *m/z* and 260.0640 *m/z* are currently unidentified.

Results From All 36 Compounds. Having validated that the pooling strategy allowed for generation and detection of all predicted major metabolites from well-characterized compounds, we searched for potential metabolites of all 36 compounds based on several criteria: 1) the *m/z* feature should appear only in pools containing the associated parent compounds, 2) the same *m/z* feature should appear in both independent

	Bupropion	(S,S or R,R) Hydroxy Bupropion	Dihydroxy bupropion
m/z (M+H)	240.1139	256.1091	272.1036
RT (min)	1.04	1.14	1.36

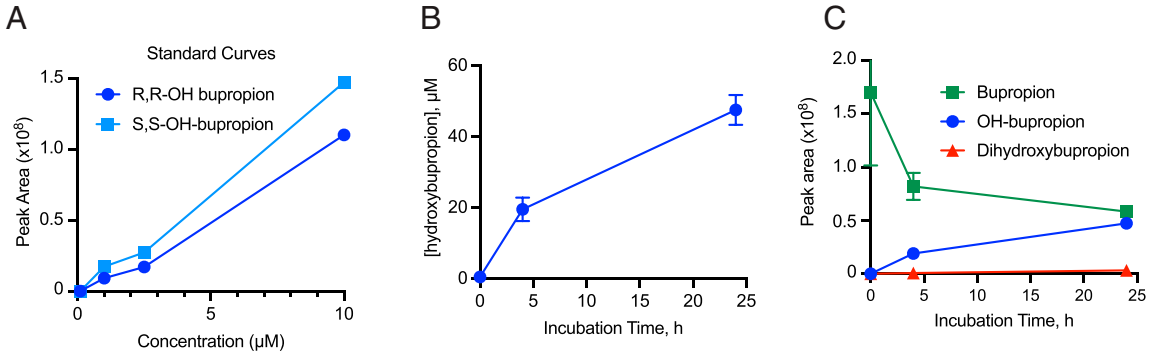

Fig. 3. Estimation of hydroxybupropion generation by the Huh7-2B6V5 cell line. Huh7-2B6V5 cells were plated on 24-well plates at 80% confluency and then two days later, media (10% FBS/PS/DMEM) containing 100 mM of bupropion was added for various incubation times. After incubation of substrate, 3 volumes of ACN were added and the plate was frozen and thawed. Cells were broken by pipetting and after spinning down the cell-media mixtures, supernatants were collected to vials for the HRMS analysis (Orbitrap ID-X Tribrid MS). (A) Standard curve of S,S-hydroxy and R,R-hydroxy bupropion. (B) Quantitation of hydroxy bupropion generation using the R,R-hydroxy bupropion standard. Values are the means ± S.D. of three individual wells from the same cell preparation. C. Detection of bupropion, hydroxy and di-hydroxy bupropion signals at indicated times from the same experiment as in panel B.

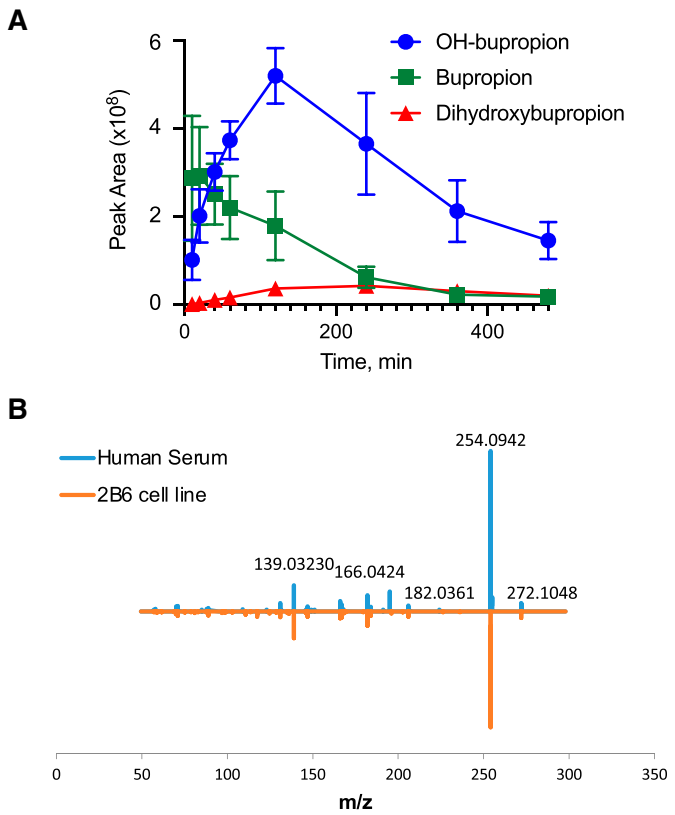

Fig. 4. Pharmacokinetics of bupropion and its metabolites, hydroxy and dihydroxybupropion from C57BL mouse after bupropion oral gavage. (A) The data for bupropion was published previously (Mimche et al., 2019), and the feature tables were reanalyzed to identify hydroxy and dihydroxybupropion based on their retention times, *m/z* values, and MS^2 spectra. Values are means ± S.D. of 5 mice in each group. (B) Mass fragmentation spectra of 272.1048 *m/z* (dihydroxybupropion) in 2B6 cell line (red) and in human sample (blue) with documented bupropion use.

pools containing the same parent compound, 3) the *m/z* in both pools should show the same cell line specificity, and 4) the intensity for respective *m/z* features should show significantly lower levels or zero values in 0 hour samples. Once we identified *m/z* based on these criteria, we annotated targeted metabolites using BioTransformer and a curated list of known mass differences caused by xenobiotic transformations (see *Materials and Methods*). Where possible, we confirmed reactions from literature searches.

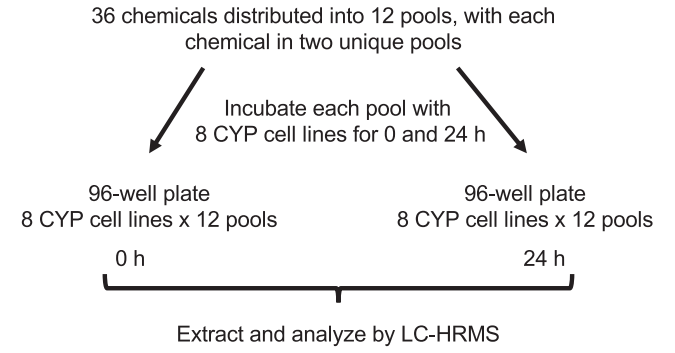

Fig. 5. Pooling strategy. (A) Pooling samples. A total of 36 compounds were grouped into 12 pools, with each pool containing a unique combination of 6 compounds and each compound being present in two separate pools. Each chemical was present at a final concentration of 20 μM in 0.1% dimethylsulfoxide. (B) Experimental design. After each pool was incubated with 8 P450-expressing cell lines for 0 and 2 hours on two 96-well plates, respectively, reactions were quenched with 3 volumes of ACN and then analyzed by LC-HRMS (Orbitrap Fusion Tribrid Mass Spectrometer). For additional details concerning cell lines and xenobiotic pools, see Supplemental Fig. 3.

Table 1 summarizes the cell-line–dependent production of metabolites from the 36 compounds detected by HILIC positive ESI. Supplemental Table 2 shows the metabolite generation analyzed on C18 negative ESI. We identified many expected metabolites and hundreds of other *m/z* features that could represent uncharacterized metabolites generated from various compounds in a cell-line–specific manner. From 36 compounds, these cell lines generated a total of 825 unidentified mass spectral signals in HILIC positive ESI mode, suggesting that this high-throughput approach could be applied systematically to identify uncharacterized biotransformation products of drugs and environmental chemicals that are generated by specific human P450 enzymes.

Discussion

Here, we demonstrate the generation of Huh7 hepatoma cell lines with stable expression of catalytically active, C-terminally-tagged P450 enzymes and demonstrate their substrate-specific P450 activities. By combining targeted mass spectral searching for known and expected metabolic products with powerful nontargeted LC-HRMS methods, we obtained evidence for a large number of uncharacterized metabolic products from common xenobiotics. It is likely that some of the of the unidentified features are not metabolites of the incubated xenobiotic: for example, they could be impurities or metabolites of impurities in the supplied chemical, or they could be products of altered cell physiology caused by the xenobiotic. The latter concern is mitigated to some extent by the fact that each identified feature is detected only in a subset of cell lines expressing specific enzymes. We further showed that LC-HRMS has sufficient specificity and sensitivity to support a mixtures approach for metabolite detection. Specifically, incubation of six compounds together in each cell line increased analytical throughput by a factor of six, helping overcome throughput on the mass spectrometer as a bottleneck to large-scale characterization of xenobiotic metabolism. Using this approach, we show that these cell lines generate metabolites from the mixtures in a cell line and substrate-specific manner, allowing for specific P450 enzyme-substrate pairs to be identified.

We have previously shown that S9 enzymes can be used to provide a high-throughput approach to generate Phase I and II metabolites to identify xenobiotic exposures in humans (Liu et al., 2021). The P450 cell lines provide a complementary workflow for simultaneous generation of Phase I, P450-dependent, metabolites of xenobiotics, and subsequent identification of active enzyme-substrate pairs. This capability to link substrates and specific metabolites with specific P450 cell lines could potentially be used for metabolic phenotyping studies in humans. This study shows that these P450 cell lines generate metabolites that are detected in human and experimental samples but not generated by the liver S9 supernatants. For example, bupropion hydroxylation by CYP2B6 is well documented (Hsyu et al., 1997; Hesse et al., 2000). Our data show that bupropion is hydroxylated in a CYP2B6 cell-line–dependent manner and that this specific cell line also generated dihydroxybupropion (RT 1.39 minutes), which was not detected previously using the S9 system (data not shown). Petsalo et al., (2007) first identified dihydroxybupropion in human urine samples using LC/MS/MS (Petsalo et al., 2007). Our data suggest that dihydroxybupropion is produced mainly through the activity of CYP2B6.

Other results show that the P450-expressing cells have activities expected for specific P450 enzymes. Omeprazole is metabolized mainly by CYP2C19 and CYP3A4 (Yamazaki et al., 1997; Li et al., 2005) and detected products as well as relative intensities of products are consistent with previous studies (Li et al., 2005; Ryu et al., 2014) showing selective hydroxylation of omeprazole by CYP2C19 and CYP3A4. Similarly, our results showing the deethylation of ethoxyresorufin by

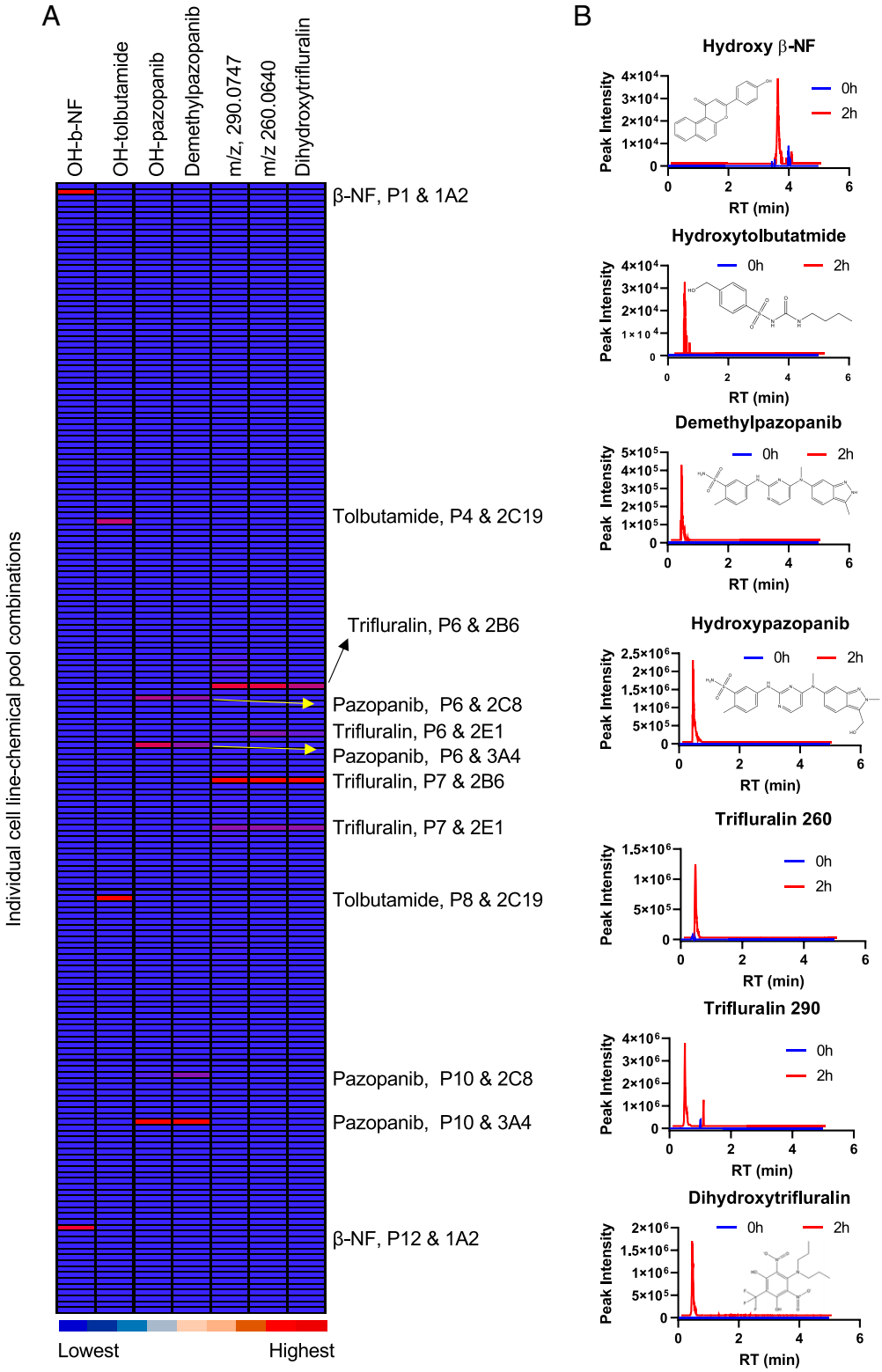

Fig. 6. Results of the pooled chemical screen for 4 selected compounds. Each pool was incubated with P450-expressing cell lines for 0 and 2 hours and quenched with ACN. Each sample was injected into HRMS as duplicate technical replicates and the signal was averaged. Each row corresponds to the average of technical replicates from individual cells. To increase the analytical stringency, a signal was removed if it was absent in one technical replicate. The same criteria as in Fig. 2 were used to select signals. (A) Heat map of metabolites from 4 selected compounds. Note that for each individual metabolite, the color scale was adjusted to show the highest signal in the well with the highest detector response for that metabolite. OH-tolbutamide was detected in C18 negative mode. The OH-tolbutamide signal was detected in pools 4 and 8 containing the parent tolbutamide after 2 hours incubation with the CYP2C19 cell line. Desmethyl and hydroxypazopanib signals were detected in pools 6 and 10 containing the parent pazopanib after 2 hours incubation with the CYP2C8 and CYP3A4 cell lines (HILIC positive mode). The OH-*β*-NF signal was detected in pools 1 and 12 containing the parent *β*-NF after 2 hours incubation with the CYP1A2 cell line (C18 negative mode). Hydroxytrifluralin and two unidentified *m/z* were detected in HILIC positive mode. These signals were detected in pools 6 and 7 containing the parent trifluralin after 2 hours incubation with the CYP2B6 and CYP2E1 cell lines. (B) Chromatograms of metabolites. From top to bottom: OH-*β*-NF, OH-tolbutamide, desmethyl and hydroxypazopanib, unidentified trifluralin metabolite 260, unidentified trifluralin metabolite 290, dihydroxytrifluralin.

TABLE 1

Xenobiotic biotransformation products from P450 cell lines

Metabolites detected in HILIC-positive mode are shown. Targeted metabolites are named. Numbers in parentheses represent unidentified biotransformation products which were strongly associated with parent compounds and identified by the criteria stated in the text. (Pearson coefficient > 0.85).

P450 Cell Line	1A2	2A6	2B6	2C8	2C19	2E1	2D6	3A4
Acenaphthene								(4)
Fluoranthene	(7)	(56)	(16)	(58)	(7)	(37)	(7)	(14)
1,1,2,2-Tetrachloroethane	(2)		(2)	(1)				
Azinphos methyl		(1)		(4)	(6)	(1)	(3)	
s,s,s, tributylphosphoro-trithioate	(3)		(2)	(1)	(2)	(3)	(4)	(2)
β-naphthoflavone	di-OH (3)			(1)				
Chlorzoxazone	(2)	(1)	(1)	(1)				(2)
1,2-diphenyl hydrazine	(1)	(1)	(1)	(3)		(1)		
N-Nitrosodipropylamine	(1)		(1)	(2)	(3)			
Dexamethasone		R (1)		R (1)		R (2)	R (1)	R (1)
Bromodichloromethane	(1)	(1)			(1)		(1)	
1,2-dichlorobenzene		(1)						
Acetaminophen	(6)	(4)	(4)	(8)	(3)		(5)	(2)
Ethylbenzene								
Benzo[a]pyrene		(1)			(1)			
Bupropion		DA (1)	OH (1)	(2)		(1)	(1)	
Ethion	(2)	(1)	(5)	(4)	(15)			(5)
Vandetanib	MK (5)	(1)	(11)	(13)	(6)	(1)	(4)	(2)
Naphthalene				(1)				(4)
Tolbutamide	(6)	(2)	(7)	(4)	OH (10)	(1)	(9)	(8)
2-Methyl naphthalene	(1)				(1)		(1)	(1)
Geneticin	(1)				(3)	(1)		
Benzo-b-fluoranthene	(1)		(1)	(2)				
DDD			(3)		(1)			(1)
Coumarin	(4)	(13)		(1)	(2)	(1)	(1)	
2,4,6-Trichlorophenol								
Endrin aldehyde		(1)						
Caffeine	(3)		(1)	(1)	(3)		(5)	(1)
Bis-2-ethylhexyl-phthalate	(3)	(6)	(5)	(2)	(3)	(3)		(5)
Nicotine	(3)	(4)	+Ch3 ?, OH, di-OH, MK, R? (1)		+Ch3 ? (1)	+Ch3 ? (1)		+Ch3 ? (2)
Trifluralin	(1)		(7)	(1)		OH, di-OH, R? (6)	(1)	(13)
Estrone	(3)							
Auranofin	(16)	(18)	(16)	(24)	(27)	(21)	(27)	(32)
Pazopanib	(1)			OH (2 RTs) (5)		(2)	(2)	H, DA (4)
Crizotinib	(3)	16	(6)	(2)	(1)	(2)		(7)
Warfarin	(2)	(2)	(1)	(3)	(3)	(5)	(3)	(1)

+CH3, methylation; DA, dealkylation; DDD, o,p'- dichlorodiphenyldichloroethane; di-OH, dihydroxylation; MK, methylene to ketone; OH, hydroxylation; R, reduction.

CYP1A2 cells, coumarin hydroxylation by CYP2A6 cells (Ghosal et al., 2003) and dextromethorphan demethylation by CYP2D6 cells (Yu and Haining, 2001) are consistent with known specificities of these enzymes. cDNA-transfected (Crespi et al., 1985; Crespi et al., 1990; Chen et al., 1997) and chemically differentiated (Choi et al., 2009) cell lines have been well characterized for expression of active P450 enzymes, and could potentially be used in the workflows we have described here and in our previous work (Liu et al., 2021). However, the ease of generation via lentiviral transduction and selection, and the introduction of a C-terminal V5 peptide tag that allows for specific immunodetection and immunoprecipitation of the enzyme (Park et al., 2017; Cerrone et al., 2020; Lee et al., 2020) makes the cells described here attractive for this and other uses. The robust metabolite generation suggests that they could be used as an alternative to other approaches, e.g. baculosomes, for enzyme phenotyping and prediction of drug–drug interactions. In principle, the approach can be extended to develop additional P450-expressing lines and cells expressing UDP-glucuronosyltransferases and sulfotransferases. The cell lines provide several advantages including: 1) ease of propagation and preservation under liquid nitrogen; 2) use without expensive and unstable cofactors such as NADPH, 3′-phosphoadenosine-5′-phosphosulfate and uridine diphosphate-glucuronic acid; and 3) metabolic product formation in a cell environment representative of the native cellular environment in vivo.

The cell lines can also be used to generate specific metabolites in quantities for more conclusive identification by MS/MS and NMR spectroscopy. For example, we identified three major metabolites of trifluralin in CYP2B6 cell lines (Fig. 6). One metabolite was proposed to be dihydroxytrifluralin from MS/MS spectra; however, two other metabolites could not be identified by their MS/MS fragmentation patterns. Batch cultures of the CYP2B6 cell line with trifluralin suggest that sufficient quantities of products can be produced for purification and analysis by NMR to elucidate structures (manuscript in preparation). In addition, these cell lines can be used for studies on the toxicity of a chemical and its metabolites, analogous to those of Chen et al. (1997) who used a P450-expressing HepG2 cell line to study liver toxicity by amiodarone and dronedarone.

We learned that a mixtures approach (6 substrates per cell line per incubation) could be used to increase throughput for these large-scale screens, reducing the number of samples to be analyzed by a factor of 1/6 in this case. To analyze 36 individual compounds in duplicate with 8 different cell lines at 0 and 24 hours would require $8 \times 2 \times 2 \times 36 = 1152$ samples for LC/MS/MS analysis. By pooling (grouping 6 compounds as one pool) and adding each compound into two different pools, we reduced the number of samples for LC/MS/MS analysis to 192, significantly decreasing expense and increasing throughput. Requiring that a mass spectral signal be generated by a P450 cell line with two different pools containing a given xenobiotic increased stringency for qualifying a feature as a metabolite from that xenobiotic. Thus, the pooling strategy can be

used as an initial screen to identify enzyme-compound–specific activity pairs and to guide subsequent metabolite generation and characterization.

This mixtures approach could be vulnerable to confounding effects of potential substrate inhibition or competition among xenobiotics in a given pool. The likelihood of such interactions is mitigated to some extent by including each chemical in two different pools, and in this particular screen we did observe some instances where the amount of metabolite produced in two different pools containing the same compound were different. However, the appearance of metabolite in the two different pools still enabled the identification of the metabolites and the enzyme(s) that produced them. One could overcome this potential disadvantage using a "post-pooling strategy" in which individual chemicals are incubated with each cell line and then cell lysates and media are pooled for LC-HRMS analysis. However, this strategy requires more biological incubations, and samples may need to be further concentrated to generate similar levels of signal as the prepooling strategy described here. Additional limitations are that impure xenobiotic preparations can complicate interpretations with a mixtures approach, and reactive products from one xenobiotic could react with other xenobiotics. While the combination of xenobiotics in different pools protects against the latter complication, the problem of impurities is always present in drug metabolism research. On a positive side, the approach as developed is well suited for systematic P450 metabolism studies of drug formulations and compounded drug mixtures.

In conclusion, we have demonstrated that cell lines that stably express xenobiotic enzymes can be used for the efficient generation xenobiotic metabolites using a mixtures approach. These cell lines are easy to maintain, easy to grow, and express high levels of active enzyme and have many potential applications. Not only can these cell lines be used to accelerate characterization and identification of xenobiotic exposures from human exposomics studies, but they can also be used for studying individual cytochrome P450-mediated drug metabolism, identifying drug–drug interactions, and also for mechanistic toxicology.

Authorship contributions

Participated in research design: Lee, Liu, Singer, Miller, Li, Jones, Morgan.

Conducted experiments: Lee, Liu, Singer.

Performed data analysis: Lee, Liu, Singer.

Wrote or contributed to the writing of the manuscript: Lee, Liu, Singer, Miller, Li, Jones, Morgan.

References

Blaženović I, Kind T, Sa MR, Ji J, Vaniya A, Wancewicz B, Roberts BS, Torbašinović H, Lee T, Mehta SS, et al. (2019) Structure Annotation of All Mass Spectra in Untargeted Metabolomics. *Anal Chem* **91**:2155–2162.

Cerny MA (2016) Prevalence of non-cytochrome p450-mediated metabolism in food and drug administration-approved oral and intravenous drugs: 2006-2015. *Drug Metab Dispos* **44**:1246–1252.

Cerrone Jr J, Lee CM, Mi T, and Morgan ET (2020) Nitric oxide mediated degradation of CYP2A6 via the ubiquitin-proteasome pathway in human hepatoma cells. *Drug Metab Dispos* **48**:544–552.

Chen L, Buters JT, Hardwick JP, Tamura S, Penman BW, Gonzalez FJ, and Crespi CL (1997) Coexpression of cytochrome P4502A6 and human NADPH-P450 oxidoreductase in the baculovirus system. *Drug Metab Dispos* **25**:399–405.

Choi S, Sainz Jr B, Corcoran P, Uprichard S, and Jeong H (2009) Characterization of increased drug metabolism activity in dimethyl sulfoxide (DMSO)-treated Huh7 hepatoma cells. *Xenobiotica* **39**:205–217.

Crespi CL, Altman JD, and Marletta MA (1985) Xenobiotic metabolism and mutation in a human lymphoblastoid cell line. *Chem Biol Interact* **53**:257–271.

Crespi CL, Langenbach R, and Penman BW (1990) The development of a panel of human cell lines expressing specific human cytochrome P450 cDNAs. *Prog Clin Biol Res* **340B**:97–106.

Djoumbou-Feunang Y, Fiamoncini J, Gil-de-la-Fuente A, Greiner R, Manach C, and Wishart DS (2019) BioTransformer: a comprehensive computational tool for small molecule metabolism prediction and metabolite identification. *J Cheminform* **11**:2.

Donato MT, Jiménez N, Castell JV, and Gómez-Lechón MJ (2004) Fluorescence-based assays for screening nine cytochrome P450 (P450) activities in intact cells expressing individual human P450 enzymes. *Drug Metab Dispos* **32**:699–706.

Ghosal A, Hapangama N, Yuan Y, Lu X, Horne D, Patrick JE, and Zbaida S (2003) Rapid determination of enzyme activities of recombinant human cytochromes P450, human liver microsomes and hepatocytes. *Biopharm Drug Dispos* **24**:375–384.

Hesse LM, Venkatakrishnan K, Court MH, von Moltke LL, Duan SX, Shader RI, and Greenblatt DJ (2000) CYP2B6 mediates the in vitro hydroxylation of bupropion: potential drug interactions with other antidepressants. *Drug Metab Dispos* **28**:1176–1183.

Hsyu PH, Singh A, Giargiari TD, Dunn JA, Ascher JA, and Johnston JA (1997) Pharmacokinetics of bupropion and its metabolites in cigarette smokers versus nonsmokers. *J Clin Pharmacol* **37**:737–743.

Jones DP (2016) Sequencing the exposome: A call to action. *Toxicol Rep* **3**:29–45.

Keisner SV and Shah SR (2011) Pazopanib: the newest tyrosine kinase inhibitor for the treatment of advanced or metastatic renal cell carcinoma. *Drugs* **71**:443–454.

Lee CM, Wilderman PR, Park JW, Murphy TJ, and Morgan ET (2020) Tyrosine nitration contributes to nitric oxide-stimulated degradation of CYP2B6. *Mol Pharmacol* **98**:267–279.

Li X-Q, Weidolf L, Simonsson R, and Andersson TB (2005) Enantiomer/enantiomer interactions between the S- and R- isomers of omeprazole in human cytochrome P450 enzymes: major role of CYP2C19 and CYP3A4. *J Pharmacol Exp Ther* **315**:777–787.

Li XQ, Björkman A, Andersson TB, Ridderström M, and Masimirembwa CM (2002) Amodiaquine clearance and its metabolism to N-desethylamodiaquine is mediated by CYP2C8: a new high affinity and turnover enzyme-specific probe substrate. *J Pharmacol Exp Ther* **300**:399–407.

Liu KH, Lee CM, Singer G, Bais P, Castellanos F, Woodworth MH, Ziegler TR, Kraft CS, Miller GW, Li S, et al. (2021) Large scale enzyme based xenobiotic identification for exposomics. *Nat Commun* **12**:5418.

Mimche SM, Lee CM, Liu KH, Mimche PN, Harvey RD, Murphy TJ, Nyagode BA, Jones DP, Lamb TJ, and Morgan ET (2019) A non-lethal malarial infection results in reduced drug metabolizing enzyme expression and drug clearance in mice. *Malar J* **18**:234.

Nebert DW, Wikvall K, and Miller WL (2013) Human cytochromes P450 in health and disease. *Philos Trans R Soc Lond B Biol Sci* **368**:20120431.

Park JW, Byrd A, Lee CM, and Morgan ET (2017) Nitric oxide stimulates cellular degradation of human CYP51A1, the highly conserved lanosterol 14α-demethylase. *Biochem J* **474**:3241–3252.

Pelkonen O, Rautio A, Raunio H, and Pasanen M (2000) CYP2A6: a human coumarin 7-hydroxylase. *Toxicology* **144**:139–147.

Petsalo A, Turpeinen M, and Tolonen A (2007) Identification of bupropion urinary metabolites by liquid chromatography/mass spectrometry. *Rapid Commun Mass Spectrom* **21**:2547–2554.

Pluskal T, Castillo S, Villar-Briones A, and Orešič M (2010) MZmine 2: modular framework for processing, visualizing, and analyzing mass spectrometry-based molecular profile data. *BMC Bioinformatics* **11**:395.

Ryu SH, Park B-Y, Kim S-Y, Park S-H, Jung H-J, Park M, Park KD, Ahn T, Kang H-S, and Yun C-H (2014) Regioselective hydroxylation of omeprazole enantiomers by bacterial CYP102A1 mutants. *Drug Metab Dispos* **42**:1493–1497.

Uppal K, Walker DI, and Jones DP (2017) xMSannotator: an R package for network-based annotation of high-resolution metabolomics data. *Anal Chem* **89**:1063–1067.

Uppal K, Walker DI, Liu K, Li S, Go YM, and Jones DP (2016) Computational metabolomics: a framework for the million metabolome. *Chem Res Toxicol* **29**:1956–1975.

Wester MR, Lasker JM, Johnson EF, and Raucy JL (2000) CYP2C19 participates in tolbutamide hydroxylation by human liver microsomes. *Drug Metab Dispos* **28**:354–359.

Yamazaki H, Inoue K, Shaw PM, Checovich WJ, Guengerich FP, and Shimada T (1997) Different contributions of cytochrome P450 2C19 and 3A4 in the oxidation of omeprazole by human liver microsomes: effects of contents of these two forms in individual human samples. *J Pharmacol Exp Ther* **283**:434–442.

Yu A and Haining RL (2001) Comparative contribution to dextromethorphan metabolism by cytochrome P450 isoforms in vitro: can dextromethorphan be used as a dual probe for both CTP2D6 and CYP3A activities? *Drug Metab Dispos* **29**:1514–1520.

Address correspondence to: Dr. Edward T. Morgan, Department of Pharmacology and Chemical Biology, Emory University School of Medicine, 5119 Rollins Research Center, 1510 Clifton Road, Atlanta, GA 30322. E-mail: etmorga@emory.edu; or Dr. Dean P. Jones, Clinical Biomarkers Laboratory, Department of Medicine, Emory University, Atlanta, Georgia 30322. E-mail: dpjones@emory.edu